



KEK Preprint 2001-108  
September 2001  
A

## SPring-8 Compact SASE Source (SCSS)

T. SHINTAKE, H. MATSUMOTO, T. ISHIKAWA and H. KITAMURA

*Submitted to SPIE's 46th Annual Meeting, The International Symposium  
on Optical Science and Technology, San Diego, California, U.S.A., July 29 - August 3, 2001*



High Energy Accelerator Research Organization

## **High Energy Accelerator Research Organization (KEK)**

KEK Reports are available from:

Information Resources Division  
High Energy Accelerator Research Organization (KEK)  
1-1 Oho, Tsukuba-shi  
Ibaraki-ken, 305-0801  
JAPAN

Phone: +81-298-64-5137  
Fax: +81-298-64-4604  
E-mail: [irdpub@mail.kek.jp](mailto:irdpub@mail.kek.jp)  
Internet: <http://www.kek.jp>

## SPring-8 Compact SASE Source (SCSS)

Tsumoru Shintake<sup>\*a</sup>, Hiroshi Matsumoto<sup>a</sup>, Tetsuya Ishikawa<sup>b</sup> and Hideo Kitamura<sup>\*\*b</sup>

<sup>a</sup>High Energy Accelerator Research Organization

<sup>b</sup>Harima Institute, RIKEN, SPring-8

### ABSTRACT

The SPring-8 Compact SASE Source (SCSS) is a high peak-brilliance soft X-ray free electron laser project. It has been funded in April 2001, aiming to generate first light in 2003 at VUV region, and ultimately 3.6 nm in water-window in 2005. Combination of the high-gradient C-band accelerator and in-vacuum short-period undulator realizes a SASE-FEL facility to generate soft X-ray within 100 m machine length. SCSS will provide six order of magnitude peak-brilliance enhancement compared to the current third-generation sources at 3 ~ 20 nm range.

### 1. PROJECT OVERVIEW

The SCSS will be constructed at SPring-8 site supported by multi-laboratory collaboration including JASRI, JAERI, KEK and RIKEN. Figure 2 shows the milestone of SCSS project. In 2001 April, the SCSS has been funded as the second phase of the long term R&D program at RIKEN to establish technology for generation and handling of high brightness radiations at SPring-8. In the first phase program, the 27 m long in-vacuum undulator was developed and it was installed into the 30-m straight-section in the 8-GeV main ring at SPring-8 and commissioned successfully last year<sup>[1]</sup>.

We will start fabrication of accelerator components in 2001, and install them into the accelerator tunnel before 2003. When half of the main accelerators and undulators are installed, we will commission the machine operation to debug the system. We start to operate SASE-FEL at visible light first, then UV and

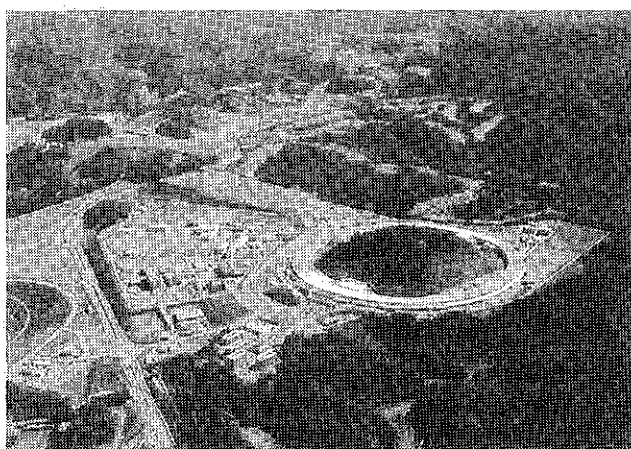


Fig. 1. SCSS will be built at SPring-8.

eventually VUV near 10 nm. When installation of whole accelerators and undulators are completed, we try lasing below 10 nm. The available shortest wavelength in SCSS will be 3.6 nm.

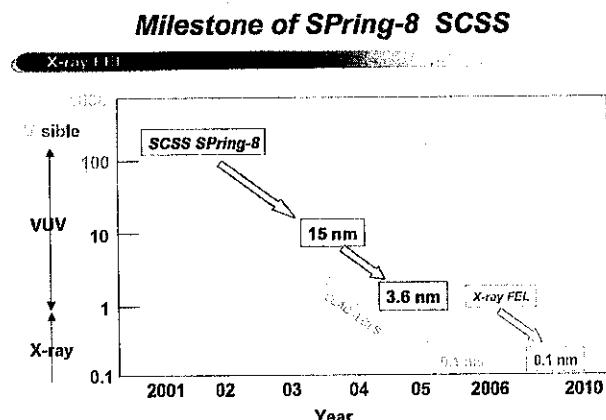


Fig. 2. Milestone of SCSS. The first light is scheduled at the end of 2003. We expect a X-ray FEL project after completing SCSS.

Figure 3 shows the spectral peak-brilliance of various proposed projects<sup>[2,3,4,5]</sup>. In design, they promise several orders of magnitude brighter light than the brightest light from various undulators in existing 3<sup>rd</sup> generation light sources. However, as seen in the experimentally achieved data points, actual machine performances are still lower than expected. It suggests the actual electron beam qualities are different from that we expected. Therefore, it is worthwhile to start our project as midway to the X-ray FEL, that is, the radiation wavelength being few-nm or longer range. Through the SCSS design and construction and beam test, we will learn much technical information, which will be very useful to realize the X-ray FEL in future. It will take almost ten years from now.

\*tsumoru.shintake@kek.jp; fax: +81-298-64-5295; http://c-band.kek.jp; High Energy Accelerator Research Organization, 1-1 Oho, Tsukuba, Ibaraki Japan; \*\*kitamura@spring8.or.jp; fax: +81-791-58-2810; The Institute of Physical and Chemical Research Kohto 1-1-1, Mikazuki-cho, Sayo-gun, Hyogo, 679-5143, Japan

## 2. MACHINE OVERVIEW

The key technologies in SCSS are

- (1) In-vacuum short-period undulator.
- (2) High gradient C-band accelerator.
- (3) Low emittance beam injector.

The radiation wavelength from a high-energy electron beam passing through an undulator is related to the beam energy and undulator period as

$$\lambda_x = \frac{\lambda_u}{2\gamma^2} \left( 1 + \frac{K^2}{2} \right). \quad (1)$$

The FEL gain length is given by

$$L_{g,1D} = \frac{\lambda_u}{4\pi\sqrt{3}\rho}, \quad (2),$$

$$\rho = \left[ \left( \frac{I_{pk}}{I_A} \right) \left( \frac{\lambda_u K (J_0 - J_1)}{2\sqrt{2\pi}\sigma_x} \right)^2 \left( \frac{1}{2\gamma_0} \right)^3 \right]^{1/3}, \quad (3)$$

where  $\rho$  is the FEL parameter,  $I_{pk}$  is the peak beam current,  $I_A$  is the Alfvén current and  $\sigma_x$  is the rms beam size.

Firstly, we adopt a design of short-period undulators, which makes the FEL gain length much shorter as seen in eq. (2) as well as lowers the required electron beam energy by eq. (1), resulting in short accelerator. Therefore the short-period undulator is quite desirable to SASE type FEL. As discussed detail in later sections, to obtain enough K-value in the short period undulator, the gap size of undulator magnets becomes narrower and sacrifices the beam clearance. The in-vacuum undulator eliminating vacuum vessel, and provides wide beam channel. Even though, to obtain enough undulator field at shorter undulator period, the gap size becomes smaller, it causes a higher resistive impedance, which deteriorates FEL gain due to the longitudinal energy spread created on short bunch. We chose 15 mm undulator period after compromising the field intensity and the resistive impedance. At the maximum beam energy of 1 GeV, the radiation wavelength becomes 3.6 nm for K-value of 1.3, which is within the water-window spectrum useful to observe wet organic materials.

Secondly, we employ the high gradient C-band accelerator, which has been developed in the R&D program carried out at KEK aiming to develop accelerator technology for future  $e^+e^-$  Linear Collider at 500 GeV c.m. energy or higher. Combination of 50 MW C-band pulse klystron and RF pulse compressor make possible to generate accelerating gradient at 31 MV/m for multi-bunch and 40 MV/m for single bunch. With this gradient, we obtain 1 GeV beam within the accelerator length less than 30 m long.

Equations (1) to (3) do not take into account the beam divergence effect due to the finite emittance. To keep saturate FEL with practical beam, the electron beam emittance is requested to be smaller than or on the order of the radiation wavelength. This provide a constraint on the beam emittance as

$$\varepsilon_n < \gamma \frac{\lambda_x}{4\pi} \quad (4)$$

The short-period undulator lowers the drive beam energy, in contrast, it lowers the required beam emittance. In SCSS, at 3.6 nm radiation wavelength, the normalized emittance of the order of  $0.6 \pi \text{mm.mrad}$  is ideal. In practice, a few times higher

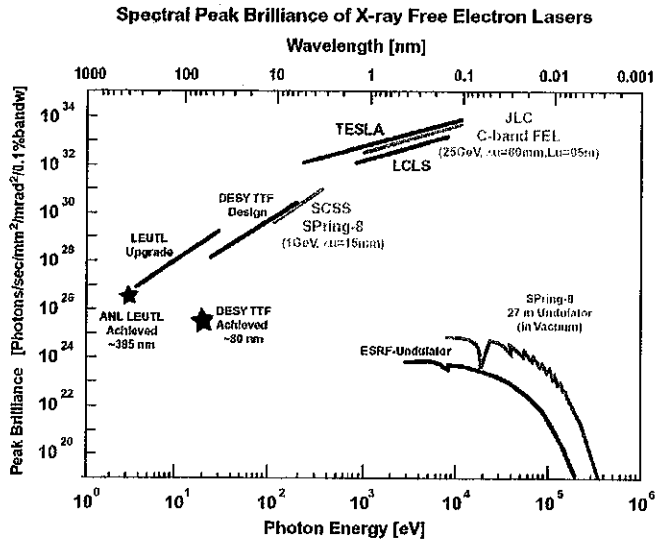


Fig. 3. Spectral peak brilliance of SASE FELs.

emittance is still acceptable, and deterioration of FEL gain is still small<sup>[6]</sup>. We designed the beam emittance as 2  $\pi$ mm.mrad. To obtain this beam emittance, we designed the low emittance beam injector using the single crystal CeB<sub>6</sub> cathode as the thermionic electron source.

Table-1 summarizes the basic SCSS parameter at 3.6 nm wavelength. We expect FEL saturation within 22.5 m long undulator. Extensive design work are now carrying out to optimize beam parameter, including the pre-buncher and buncher design, the first bunch compressor with second harmonic correction cavity, double chicane design to tolerate the CSR effect in the second bunch compressor, undulator parameter and beam control in undulator. The parameter listed in Table-1 is still tentative.

Table-1 SCSS parameters at 3.6 nm radiation wavelength.  
Note that the bunch length is denoted by FWHM value.

bunch charge	$Q$	1	nC
normalized emittance	$\epsilon_{nx,y}$	2	$\pi$ mm.mrad
final electron energy	$E$	1	GeV
final rms energy spread	$\sigma_8$	0.02	%
final FWHM bunch length	$\Delta z$	0.15	mm
	$\Delta t$	0.5	psec
peak current	$I_{pk}$	2	kA
undulator period	$\lambda_u$	15	mm
minimum gap	$g$	3.7	mm
maximum K-parameter	$K$	1.3	
undulator unit length	$L_1$	4.5	m
total undulator length		22.5	m
beta function	$\beta$	10	m
FEL parameter	$\rho$	8.9	$\times 10^{-4}$
gain length	$L_g$	0.94	m
saturation length	$L_{sat}$	20	m
saturation power	$P_{sat}$	2.0	GW

### 3. ACCELERATOR

#### 3.1 Accelerator Layout

As seen in Table-1, in order to saturate FEL at shortest wavelength in SCSS:  $\lambda_x = 3.6$  nm, we need a short bunch of 0.5 psec.FWHM, 2 kA, and 1 nC beam. This short high-peak current bunched-beam is generated in seven stages as below. Here we describe the bunch length by FWHM value rather than rms value as  $\sigma_z$ . This is because in our system the longitudinal current profile is close to square pulse. Figure 4 shows the beam line layout and beam parameter.

- (1) 300 nsec, 3A (500 keV) long pulse is generated from a high-voltage gun with thermionic cathode.
- (2) 0.33 nsec part of 3A (500 keV) is cut out from 300 nsec-pulse by means of kicker deflector and energy filter after 476 MHz sub-harmonic buncher.
- (3) 33 psec, 30A (500 keV) pulse is made by bunching after drifting 800 mm with velocity modulation applied at the 476 MHz sub-harmonic buncher.
- (4) 4 psec, 250 A (20MeV) pulse is formed by the first-stage bunch compressor using a chicane magnet. To correct 2<sup>nd</sup> order error associated with acceleration field of L-band accelerator, a C-band short accelerator is prepared right before the compressor. Compression factor is 8.
- (5) Beam is accelerated to 300 MeV with high gradient C-band accelerator (Unit-1). The maximum accelerating gradient for single bunch is 40 MV/m and energy gain is 280 MeV with 8 m long unit.
- (6) 0.5 psec, 2 kA bunch (300MeV) is formed by the second-stage bunch compressor using double-chicane configuration. The bunch compression factor is 8. To cancel emittance growth in BC2, the double chicane configuration will be used, if it is necessary.

(7) The beam is accelerated to 1 GeV (maximum energy) by three units of C-band accelerator (C-2, 3, 4), where the energy slope is corrected. The designed beam parameter in the undulator is 1 GeV, 1 nC, 2 kA. Bunch length is 0.5 psec.FWHM or 0.15 mm.FWHM, which is close to  $\sigma_z = 0.08$  mm.

### SPring-8 Compact SASE Source

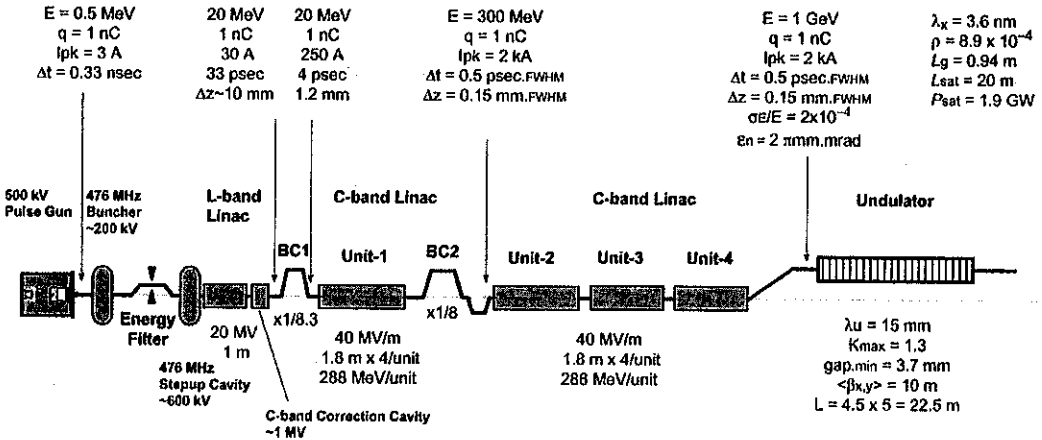


Fig. 4. Beam line layout and beam parameter.

### 3.2 Electron Injector Design

The RF-Gun is well known device as the low-emittance electron beam source, and believed to be the best choice as the electron injector for the SASE FELs at short wavelength. Since the emitted electron bunch from the photo-cathode is quickly accelerated to the relativistic energy within a short-distance, the emittance dilution due to the space charge field is minimized. Additionally, today's continuously advancing technology in laser engineering made feasible various type of pulsed laser system generating short optical bunch with fairly stable energy. Also, harmonic generation of short-wavelength radiation made possible to use the bare metallic surface as the photo-cathode, thus the lifetime becomes very long maintaining reasonably high quantum efficiency.

In the SCSS project however, we chose a high-voltage pulse-gun with thermionic-cathode, instead of RF-Gun. The beam bunching is performed by the traditional pr-buncher and buncher configuration. Major reason of this choice is its high stability and tunability.

Since SASE-FEL is still new technology and to realize X-ray laser in future we needs long-term R&D studies on theoretical and experimental aspects. To study SASE-FEL performance experimentally, a best way will be to test FEL performance by changing the beam parameter one-by-one. That is, by changing total charge and bunch length, or changing trajectory inside the undulator, we measure the saturation power change. To perform this type of study, we need a very stable injector and accelerator system, and each parameter has to be changed independently.

In the RF-gun, available beam parameter is a complicated function of many parameters, i.e. the RF-drive power level, tuning of cavity, quantum efficiency of cathode, laser timing, laser beam profile, laser beam intensity, light reflection at vacuum window, laser beam alignment, solenoid current for emittance correction, alignment of solenoid. Unfortunately, they are mixed each other in the small volume of RF-gun. Therefore, we think it will be hard to control the beam parameter one-by-one in the RF-gun based system.

Figure 5 shows the schematic diagram of the low-emittance beam injector for SCSS. We use CeB<sub>6</sub> single crystal cathode of 3 mm in diameter, from which we pull out a beam current of 3 A using 500 kV pulse voltage applied in 5 cm gap. The pulse length of beam at this point is about 1 μsec FWHM, and 300 nsec flat-top. In order to form a single bunch, we deflect the beam vertically through a beam chopper (a strip-line pulse-deflector) located after the electron gun, and scrape the unwanted

## Low Emittance Injector for SASE-FEL

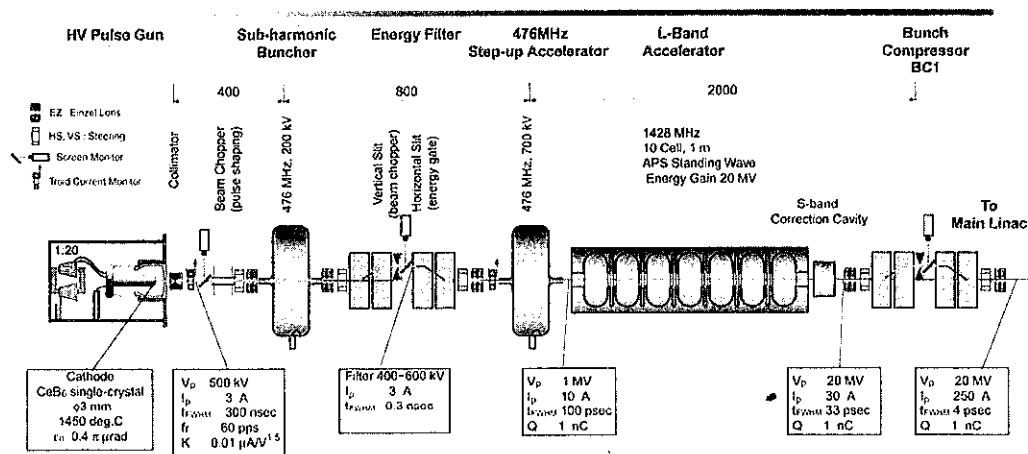


Fig.5. Low emittance beam injector.

part by a vertical slit located at the energy filter after the sub-harmonic buncher. To compress the bunch length, velocity modulation is applied at the 476 MHz sub-harmonic buncher. Top and bottom parts of the beam energy is rejected with the movable horizontal scraper located inside the energy filter. With drift-length of 800 mm, the electron beam is focused in longitudinal to a short bunch.

In this configuration, the beam parameter control becomes easier. For example, to change the bunch length without changing peak current, we move the horizontal slit inside the energy filter. To change the peak current by keeping the bunch length almost constant, we change the temperature of the cathode.

### 3.3 Electron Gun

As discussed in the previous section, we decided to use high-voltage pulse gun, rather than RF-Gun. To generate single bunch, the control grid is frequently used in traditional design. Since a very low emittance beam is requested here, we may not use the control grid. The non-uniform field around the grid deflects electron trajectory in transverse direction and deteriorates the beam emittance. Once we decided not to use the control-grid, we have to apply a pulsed high-voltage on the cathode, not the DC voltage. The pulsed voltage is also desirable to reduce probability of HV break down between cathode and anode, or flash-over along the insulating ceramic tube.

The normalized emittance due to thermal velocity of electron emitted from a hot cathode is given by

$$\epsilon_{n.rms} = \frac{r_c}{2} \sqrt{\frac{kT}{m_0 c^2}} \quad (5)$$

where  $r_c$  is the cathode radius and  $T$  is the cathode temperature in Kelvin. In the present case,  $r_c = 1.5$  mm,  $T = 1800$  K, and the beam emittance becomes  $0.4 \pi \text{mm.mrad}$ . This emittance is much lower than the design emittance:  $2 \pi \text{mm.mrad}$  at the undulator. Since the emittance dilutions happen in the buncher, the main accelerator and the bunch-compressors are mostly projected emittance growth. There is no much error source to deteriorate the slice-emittance. The SASE-FEL gain is determined by the slice-emittance, not by the projected emittance. Therefore, it is still worthwhile to use electron gun of very low emittance. Only when we account the peak brilliance, the projected emittance and correlated energy spread determine the radiation quality. To make the peak brilliance higher, lower projected emittance is desired.

The required beam current from the cathode is about 3 A, thus the current density becomes  $40 \text{ A/cm}^2$ . Cathode material which is able to emit this level of high-current density is uniquely  $\text{LaB}_6$  (lanthanum hexaboride) or  $\text{CeB}_6$  (cerium

hexaboride). For a short period, we can extract more than 40 A/cm<sup>2</sup> from Ba-oxide cathode by operating at high temperature. We chose CeB<sub>6</sub> single-crystal. CeB<sub>6</sub> has recently become familiar as the high brightness electron source for the electron microscope. It has lower work-function than LaB<sub>6</sub> and lower evaporation rate of cathode-material, resulting in longer lifetime. It is reported that in the field tests the Volgel mount CeB<sub>6</sub> cathode have lasted up to 10,000 hours in a PHI 590 Scanning Auger system<sup>[7]</sup>. CeB<sub>6</sub> also possesses better resistance to carbon contamination than LaB<sub>6</sub>.

At 1450 °C, the current density of 70 A/cm<sup>2</sup> will be available. To maintain this temperature, we need careful design of heater, support structure and radiation shield. Figure 6 shows the cathode assembly, which employs the Vogel-type cathode mount. The CeB<sub>6</sub> cathode is supported by two finger-like current-leads with a small block of pyrolytic graphite inserts, which act as heater as well as support. CeB<sub>6</sub> and LaB<sub>6</sub> cannot be supported directly by metallic structure, since boron atoms diffuse into metal at high temperature and metal becomes brittle, therefore graphite block is used.

The space-charge limited current between cathode-and-anode parallel plates is given by the following Child-Langmuire equation.

$$j_{SC} = 2.33 \times 10^{-6} \frac{V^{3/2}}{d^2} \quad (A/m^2) \quad (6)$$

In case the cathode diameter  $\phi_c$  is much smaller than the gap size  $d$ , the current limit becomes higher than eq (6). Analytical evaluation of enhancement factor has been recently made, and compared with E-GUN code simulation. Both of the analytical estimation and computer simulation predicted the enhancement factor of 4.5 in case of 3 mm diameter and 50 mm gap. Applying 500 kV, the space-charge limited current becomes 10.5 A. Therefore, we can operate the electron gun as “temperature limited condition”. In this condition, the beam current is determined by the cathode temperature, not by the gun voltage. Since the charge density near the cathode is lower than the space-charge limited condition, the electric field becomes fairly uniform over the cathode surface, and emittance dilution associated with beam spread due to space during beam acceleration to the anode becomes lower. We are analyzing this effect with analytical scaling law.

The beam emittance dilution due to the surface roughness of the cathode is important factor<sup>[8]</sup>. In 1990's, scientists led by Kobayashi at KEK Japan have studied on relation of surface quality of cathode to the beam emittance<sup>[9,10]</sup>. They developed a beam emittance measurement system. Using 150 kV pulse voltage, the beam was extracted from cathode, and filtered with “pepper pot disk” (a screen with many pin-holes). The image of those beams were observed with thin scintillator screen after traveling free-space of 17 cm. They tested LaB<sub>6</sub> single crystal of 1 mm diameter, LaB<sub>6</sub> poly-crystal, and Ba-impregnated (Bi-type Ir coated) cathode. The best equality of beam was obtained from LaB<sub>6</sub> single-crystal, the next was the Ba-impregnated cathode. The observed minimum normalized emittance was 0.94 πmm.mrad at 95% population, which corresponds to 0.3 πmm.mrad in rms normalized emittance. The worst one was the LaB<sub>6</sub> poly-crystal, this is due to the surface roughness and non-uniform emission density.

The gun voltage 500 kV was determined by considering the beam divergence due to space charge and technical issue of HV breakdown limit. Assuming cylindrical uniform beam, the beam spreading due to the transverse space-charge force is given by

$$\frac{d^2r}{dz^2} = \frac{E_r}{m_0 c^2 (\beta \gamma)^3}. \quad (7)$$

This equation indicates the space charge force can be much lowered by increasing the gun voltage. However, higher gun voltage causes higher risk of HV break down. We decided the gun voltage as 500 kV. We believe 500 kV and 1 μsec width is technically feasible, because today's super power klystrons, such as the X-band klystrons developed at SLAC uses 465 kV pulse voltage<sup>[11]</sup>, and similar klystrons developed at KEK uses 500 kV or even higher voltage, where no serious failure such as puncture of the ceramic insulator or frequent HV breakdowns inside the gun are not recently observed. Most failures are puncture of the ceramic-window in the RF-output waveguide or the output structure breakdown, or parasitic beam oscillations, they are not directly related to the high-voltage applied on the gun.

The electron gun will be assembled in a high-voltage tank filled with insulation oil. The 25 kV pulse voltage will be fed from a pulsed modulator using pulse-forming-network (PFN), through four-pair of 50 Ω cables. Using a step-up pulse transformer (ratio 1:20), the voltage will be raised to 500 kV. To make better impedance matching, a dummy resistor of

30~50 kΩ will be laded in parallel to the gun. The heater power is transferred through the bi-filar second-winding of the transformer. All of those techniques are commonly used in pulsed klystron power supply, and well established. We are now designing the hardware detail. The first beam acceleration test is scheduled in early period of 2002.

Recently, J. Haimson has developed 550 kV electron gun for a 17 GHz linac<sup>[12]</sup>, it has quite similar design as ours (except the cathode is Ba-oxide). Experimental test was made, and the rms emittance of approximately  $1.8 \pi \text{mm.mrad}$  was achieved at an energy of 440 kV with a transmitted beam of 600 mA and a pulse width of 600 nsec. This result proves this type of HV gun is very promising as a low-emittance beam injector.

### 3.4 Sub-Harmonic Buncher, Step-up Accelerator and L-band Accelerator.

When a charged particle of non-relativistic energy passes through a single cell RF cavity, it receives the radial momentum from the radial electric field near the nose-cone, and the azimuthal magnetic field. Since this kick varies with particle phase on the RF-field, the projected emittance is increased. The emittance dilution scales as:

$$\Delta\mathcal{E} \sim \frac{2\pi \Delta t}{T_{RF}} \cdot \frac{2\pi \sigma_r^2}{\lambda_{RF}} = \frac{2\pi c \Delta t \cdot 2\pi \sigma_r^2}{\lambda_{RF}^2}. \quad (8)$$

This equation indicates a lower RF frequency is desirable for low emittance injector. We chose the RF frequency of sub-harmonic buncher and step-up accelerator at 476 MHz (1/6 of S-band, 1/12 of C-band). The bunch length 0.33 nsec is much smaller than the period  $T_{RF}$  2.1 nsec, and beam radius of a few mm is much smaller than the wavelength of 600 mm. At this frequency, the IOT-tube is commercially available at 100 kW peak power level.

The step-up accelerator boosts beam energy from 400 keV to 1 MeV, before injected into L-band accelerator. With this acceleration the space charge effect is about 4 times lowered as eq. (7) and emittance dilution in the first cell of L-band accelerator is also lowered.

L-band was chosen at the buncher accelerator, because of the same reason as sub-harmonic buncher. Since the Q-factor of the cavity is high, optimum length of the traveling-wave disk-loaded structure becomes too long (~9m), we decided to use a standing-wave accelerator using alternating-period structure (APS). Using 10 MW class L-band klystron, we obtain 20 MV acceleration gain in the one meter long L-band structure. Preliminary calculation of beam emittance in the injector was performed using FCI-code<sup>[13]</sup>, and it was confirmed that the beam can be transported to the L-band accelerator with beam emittance increment less than  $0.7 \pi \text{mm.mrad}$  for 1 nC charge.

### 3.5 C-band Main Accelerator

In the SCSS current design, the main linac is the C-band high-gradient accelerator. It was originally developed as the main linear accelerator in the e<sup>+</sup>e<sup>-</sup> linear collider project in Japan<sup>[14]</sup> (Fig. 7). The frequency of C-band is 5712 MHz, which is twice higher than the conventional S-band frequency 2856 MHz. It was proposed as the optimum drive RF frequency for the e<sup>+</sup>e<sup>-</sup> Linear Collider using room-temperature accelerating-structure (not super conducting structure). Because the shunt-impedance of accelerating structure becomes 1.4 times higher at C-band than S-band, it is possible to obtain higher accelerating gradient. Figure 8 shows the system diagram. One unit consists of two 50 MW C-band klystrons and their power supply named "Smart Modulator", an RF pulse compressor and four accelerating structure. The design value of the accelerating gradient is 31 MV/m for the multi-bunch beam, and 40 MV/m for single bunch.

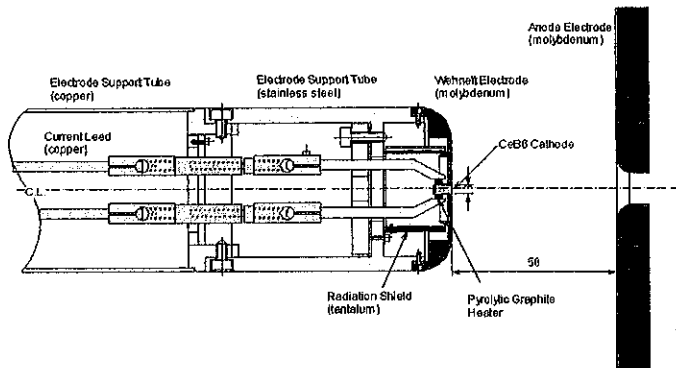


Fig. 6. The cathode assembly using CeB<sub>6</sub> single-crystal with Vogel-type mount. It is fully demountable design to ease maintenance. There is no need to focus the beam, the wehnelt electrode is made flat. We are also preparing a different type of cathode mount using cylindrical graphite heater. The cathode will be operated at near 1450 °C.

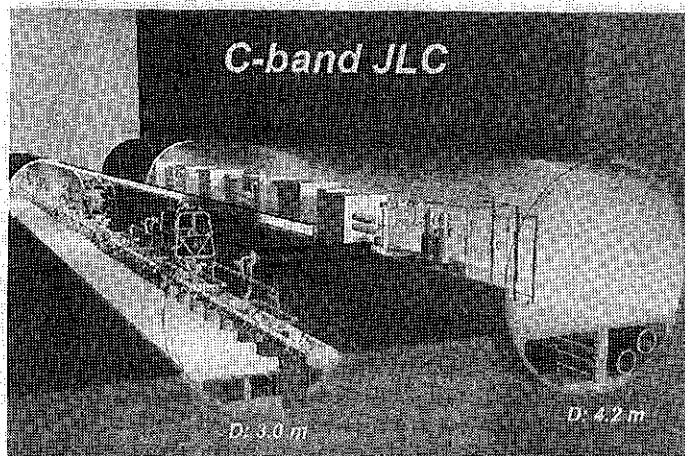


Fig. 7. The C-band main accelerator in the Japanese Liner Collider (JLC) project.

accelerating structure using choke-mode cavity. The R&D results are summarized in Table-2. The high power tests on the RF-pulse compressor and the accelerating structure have not yet been performed. Those high-power tests are scheduled in 2002.

The C-band RF system in SCSS is identical to that in the linear collider project. Therefore, construction of this 1 GeV C-band accelerator becomes a best string-test. Whole construction process: the design work, fabrication of RF components, installation to tunnel, wiring to the control system, the high power processing, and finally beam operation will provide useful information for constructing large scale  $e^+e^-$  linear collider in the future.

### 3.6 Bunch Compressors

Detail design of the bunch compression system has not yet been completed. Only outline of the design is described here.

(1) First bunch compressor at 20 MeV: BC1 (33 to 4 psec, 10 to 1.2 mm.FWHM, compression ratio 1/8.3)

The L-band accelerator (1428MHz) captures the bunch at 1 MeV. Since the bunch length inside the L-band accelerator is fairly long (~33 psec), the compressed bunch length is limited by non-linearity of the RF curvature. The C-band single cell cavity right before the BC1 is used to correct this error, and effectively generate fairly straight energy slope on the bunch. Figure 9 shows this scheme. Following linear summation provides a very flat plateau on the top of cosine curve.

$$V_c = V_0 \left[ \cos(\omega t) + \frac{1}{n^2} \cos(n\omega t) \right]. \quad (9)$$

Concerning to the safety issue on high accelerating field, we concluded the average accelerating gradient of 40 MV/m is well below the practical limit of the field emission (dark current) and structure damage due to HV breakdown<sup>[15]</sup>. Therefore, we will be able to operate the structure at this accelerating gradient for fairly long machine lifetime.

When we started hardware R&D in 1996, there were no any high-power RF-components available at C-band. Therefore, we firstly started development of a basic component, i.e., the waveguide by extruding the copper pipe. After five years R&D, we have developed the 50 MW class C-band klystrons, the Smart Modulator, the RF-pulse compressor which capable of flat-top pulse generation, and the HOM-damped

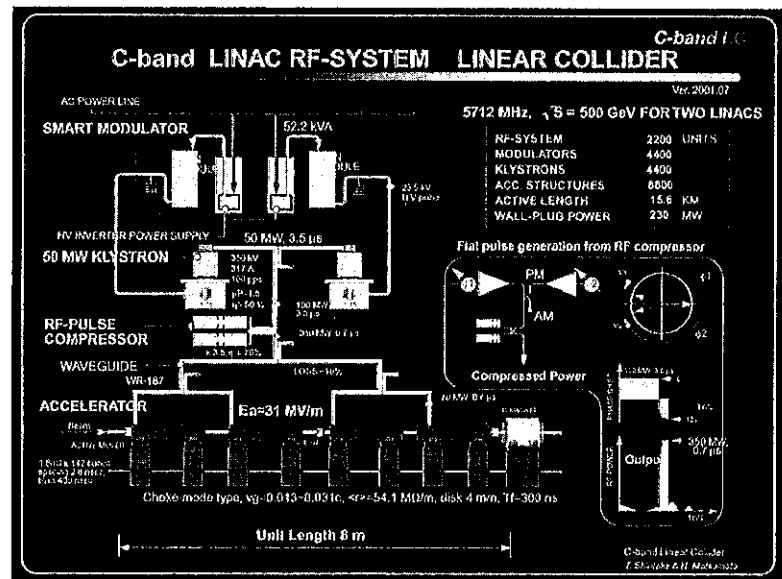


Fig. 8. C-band main linac RF-system. Exactly same system as the JLC version will be constructed in SCSS.

By adding a sin-wave on this accelerating field, we can effectively create a fairly straight energy slope on the bunch. In actual machine, the sin-wave component is not separately supplied, but effectively generated by simply shifting the fundamental rf-phase. With this correction, the bunch length is not limited due to L-band field curvature.

The coherent synchrotron radiation (CSR) effect is not a issue, since the bunch length is long enough and the shielding effect works well. Using rectangular vacuum chamber of small height, the CSR radiation is well cancelled with radiations of the mirror images on top and bottom chamber walls.

(2) Second bunch compressor at 300 MeV: BC2 (4 to 0.5 psec, 1.2 to 0.15 mm.FWHM, compression ratio 1/8.

The short bunch length can create unwanted emittance growth due to CSR. During passage in the bending magnets of chicane compressor, the coherent component of the synchrotron radiation from the tail can catch up the head particle of the bunch, and decelerate it. Due to energy loss inside the bending magnet, the particle is bent more, resulting in tilting the bunch head in horizontal direction. Therefore, the projected emittance is diluted. While the slice emittance does not change, the betatron oscillation will be created. The energy loss is linearly correlated to the longitudinal position inside the bunch, it can be corrected by off-crest acceleration in the C-band accelerator. While, CSR effect does not deteriorate the slice emittance and not affect on the FEL gain, its causes the orbit distortion inside the undulator, it differs with longitudinal position inside the bunch, and finally lowers the peak brilliance of emitted radiation. Therefore, it is necessary to maintain the projected emittance lower. The design work is undertaken now. In the case the emittance dilution is severe, the double chicane configuration will be introduced same as other projects<sup>[4]</sup>. Because the beam energy is low, the in-coherent synchrotron radiation (ISR) effect is small.

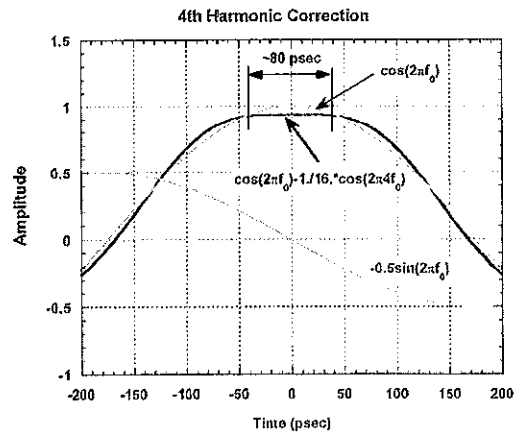


Fig. 9. Harmonic correction on L-band accelerating field with fourth harmonic C-band field. The flat top of 80 psec is wide enough for the bunch length of 33 psec.FWHM. Adding sin-wave (in practice shifting phase of L-band field), we obtain a linear slope.

#### 4. UNDULATOR

##### 4.1 In-vacuum Short-period Undulator

We use the in-vacuum short-period undulator<sup>[16]</sup>. The interior view of recently installed 27 m long undulator is shown in Fig. 10, together with schematic illustration. Because the permanent magnets are arranged in the same ultrahigh vacuum as for the storage ring, so that the vacuum gap is equal to the magnetic gap. Therefore this type has a great flexibility for operation of FEL. For example, for initial beam commissioning or machine tuning of upstream, the gap can be set a wide value, and for FEL operation we can close down to the required value. The disadvantage are that it has relatively complicated structure and needs high technical skills to construct because we have to realize ultrahigh vacuum without any demagnetization of the undulator magnets, and the fabrication of the vacuum system cannot be separated from the other parts of the device.

The first in-vacuum undulator was developed at KEK in 1992 under the leadership of Kitamura, one of the authors. Since then, he and his group of SPring-8 have continuously developed technology of this type of undulator and installed plenty of those into different storage rings<sup>[16]</sup>. At present, 19 in-vacuum undulator based on this scheme have been installed at SPring-8. The longest undulator installed is 35 m long undulator at SPring-8 and successfully commissioned its user operation last year<sup>[1]</sup>.

A short period undulator is one of the key technologies to realize compact facility of SASE-FEL as discussed in the previous section and as we sited “Compact” in the project name SCSS. The first mini-gap undulator was developed 1997 as an extension of the in vacuum undulator, under the international collaboration between NSLS and SPring-8. The period length is very short, i.e. 11 mm, and number of periods is 29. The maximum field of 0.7 T (K=0.72) is obtained at the minimum gap of 3.2 mm. The device has been successfully operated in the X-ray ring at NSLS since 1997. Therefore, technology to fabricate mini-gap in vacuum undulator is well established, at least for a short section.

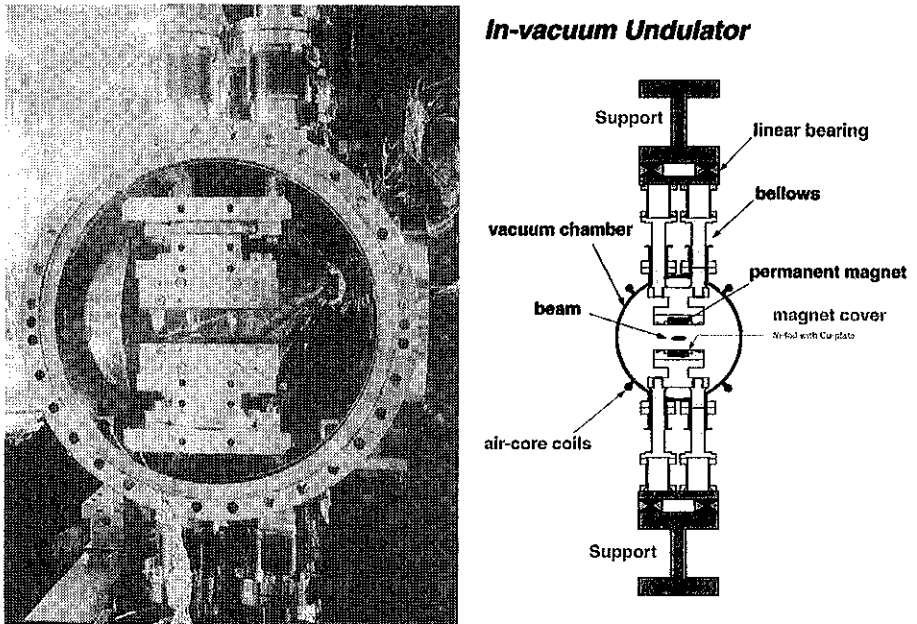


Fig. 10. Interior view of the in-vacuum undulator (left) and schematic illustration (right). Permanent magnets sit inside the vacuum vessel, and supported through vertical movable arms. There is only a thin nickel foil between the beam to the permanent magnets, and maximize the beam clearance inside gap. In order to smoothly transfer the wall current with beam, the nickel foil with copper plated is attached on the pole surface with magnetic attractive force.

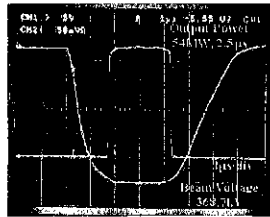
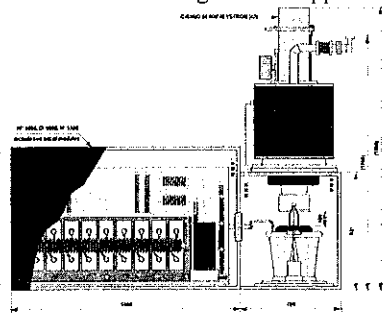
In the SCSS we need to extent this technology for a long undulator. Question is how much should be the unit-length? From the experiences of fabricating a number of in-vacuum undulators, we decided unit length as 4.5 m. We believe that it is possible to make the undulator field accurately to maintain the beam orbit distortion less than the beam size, i.e., 0.1 mm at 1 GeV. Thanks to short period of the in-vacuum undulator, the FEL gain length of SCSS is only 0.94 m as seen in Table-1, so that the optical power will be amplified by  $\exp(+4.5/0.94)=120$  times higher in one unit. Therefore, at the exit of the one unit, the fraction of the radiation power from the upstream undulator will be less than 1 %. This indicates that we do not need to care about phase-slip or alignment between two undulator-units. Brief beam simulation test was performed by GENESIS, the result supported this fact. As well known in FEL-theory, the "signal" is carried on the electron beam as the density modulation of "micro-bunch" along the undulator. This is also true when the beam is traveling the drift-section between two undulator units.

#### 4.2 Resistive Wall and Surface Roughness Impedances of Beam Pipe

When the bunch length becomes short, frequency spectrum of the beam current extends to very high frequency and the single-bunch wakefield associated with finite conductivity of beam pipe, and surface roughness can also deteriorate beam quality. Wakefield potential due to the resistive impedance for a very short bunch was analyzed by Henry and Naoply<sup>[17]</sup>. We approximately estimated the energy spread in a parallel plate gap in an undulator by simply assuming the radius being equal to half of gap and energy spread being half of the pipe case. With the bunch charge of 1 nC, and the gap size 4 mm, undulator length 20 m, the energy spread becomes lower than 0.02% for bunch size  $\sigma_z = 50\text{--}100 \mu\text{m}$  at 1 GeV. To obtain K-value higher than 1.3 at gap size near 4 mm, we decided the undulator period as 15 mm.

According to the surface roughness, recent analysis which takes into account the high aspect-ratio of surface roughness of a practical smooth-surface on commercially available metal plate, indicates that the energy spread is negligibly small enough<sup>[18]</sup>.

Table-2 Phase-I R&D summary on C-band RF-system and application to SCSS.

Items	Phase-I R&D Target	SCSS Application (Phase-II)
	Achieved Results	
Klystron	<p>Output 50 MW, Efficiency &gt;45% Pulse width &gt;2.5 <math>\mu</math>sec Pulse repetition 100 pps Focusing Power &lt; 5 kW</p> <p>All of No. 1, 2, 3 tubes achieved 50 MW output, pulse width 2.5 <math>\mu</math>sec and 50 pps. No. 3 tube showed 47% power efficiency. Focusing power 4.6kW. Life test No.2, 3 &gt; 5000 hours.</p>	<p>Refine design details for the mass-production and reducing cost. PPM-klystron is an option.</p>  <p>Example of output power.</p>
Pulse Modulator Supply	<p>350 kV, 2.5 <math>\mu</math>sec pulse generation, power efficiency &gt;50%</p> <p>Smart Modulator, No. 1 Inverter HV power supply was firstly used in klystron modulator. Operation for klystron life-test was very successful. Power efficiency &gt;52.4%</p>	<p>Oil-filled closed design will be applied.</p> 
RF Pulse Compressor	<p>Power gain &gt;3.5, Power efficiency &gt;70%</p> <p>Cold Model Test (1997) Power Gain 3.25, Efficiency 65% Not yet performed the high-power test.</p>	<p>Temperature stabilized design will be employed. Invar body with copper plating will provide better than one tenth phase-sensitivity on the temperature variation. High power test is scheduled in 2001.</p>
Accelerating Structure	<p>Multi-bunch 1.6 nC, 80 bunch Acceleration gradient &gt; 35 MV/m</p> <p>ASSET test at SLAC demonstrated damping performance of the choke-mode cavity.</p>	<p>Refine design details. Optimization for mass-production. Lowering cost. The multi-bunch option in SCSS will provide high average brightness.</p>
RF-Beam Position Monitor	<p>Resolution of RF-BPM &lt;100 nm Position accuracy &lt; 10 <math>\mu</math>m</p> <p>Resolution ~ 25 nm (FFTB test) Position accuracy &lt; 10 <math>\mu</math>m</p>	<p>Optimization for multi-bunch beam Detection circuit for multi-bunch. Damping HOM in RF-BPM.</p>

## REFERENCES

1. H. Kitamura, T. Bizen, T. Hara, X. Marechal, T. Seike and T. Tanaka, "Recent Developments of Insertion Devices at SPring-8" to be published in N.I.M.
2. Kwang-Je Kim and Zhirong Huang, "Present Status of X-ray FELs", Proc. 19<sup>th</sup> ICFA Advanced Beam Dynamics Workshop on Future Light Sources, Physics of and Science with the X-ray Free Electron Laser, Arcidosso, Italy, Sep. 10-15, 2000
3. J. Rossbach, "New Development on Free Electron Lasers Base on Self-Amplified Spontaneous Emission", Proc. PAC2001, Particle Accelerator Conference, Chicago, Illinois, June 18-22, 2001
4. P. Emma, "Issues and R&D Critical to the LCLS", Proc. PAC2001, Particle Accelerator Conference, Chicago, Illinois, June 18-22, 2001
5. S. V. Milton *et al.*, "Exponential Gain and Saturation of a Self-Amplified Spontaneous Emission Free Electron Laser", Science express, Vol. 17, May 2001
6. Ming Xie, "Design Optimization for An X-ray Free Electron Laser Driven by SLAC Linac", IEEE Proc. for PAC95, No. 95CH3584, 183, 1996
7. private communication with FEI company, 19500 NW Gibbs Drive, Suite 100, Beaverton, OR 97006-6907 USA, <http://www.feibeamtech.com>
8. Y. Y. Lau, "Effects of cathode surface roughness on the quality of electron beams", J. Appl. Phys. 61 (1), 1 January 1987.
9. H. Kobayashi *et al.*, "Emittance Measurement for High-Brightness Electron Guns", Proc. Linear Accelerator Conference, Ottawa, Canada, Aug. 23-28, 1992
10. Y. Yamazaki *et al.*, "High-precision Pepper-pot Technique for a Low-Emittance Electron Beams", Nucl. Instrum. and Methods in Physics Res. A322 (1992) pp. 139-145.
11. D. Sprehn, G. Caryotakis, K. Eppley and R. M. Phillips, "PPM Focused X-band Klystron Development at the Stanford Linear Accelerator Center", SLAC-PUB-7231, July 1996. p.9, 3<sup>rd</sup> International Workshop on RF Pulsed Power Sources for Linear Collider (RF96), Hayama, Japan, 8-12 April 1996.
12. J. Haimson, B. Mecklenburg, G. Stowell and E. L. Wright, "A Fully Demountable 550 kV Electron Gun for Low Emittance Beam Experiments with A 17 GHz Linac", Proc. 1997 IEEE Particle Accelerator Conference, 97CH36167, Vol. 3, 1997, pp. 2808-2810
13. T. Shintake, "Recent Status of FCI: PIC Simulation of Coupled Cavity Structure", Proc. 18<sup>th</sup> Int. Linac Conference, Linac96, Geneva, Switzerland, 26-30 August, 1996
14. T. Shintake, "Results from Hardware R&D on C-band RF-System for e<sup>+</sup>e<sup>-</sup> Linear Collider", Proc. XIX Int. Linac Conf. Linac98, Aug. 23-28, 1998, Chicago, Illinois, USA.
15. H. Matsumoto, "Dark Currents", Proc. 18<sup>th</sup> Int. Linac Conf., LINAC96, Geneva, Switzerland, 26-30 Aug. 1996.
16. H. Kitamura, "Recent trends of insertion-device technology for X-ray sources", J. Synchrotron Rad. (2000), 7, pp. 121-130
17. O. Henry and O. Napoly, "The resistive-pipe wake potentials for short bunches", Particle Accelerators, Vol.35, pp.235-247, 1991
18. G. Stupakov, "Surface Roughness Impedance", Physics of, and Science with, the X-ray Free Electron Laser, Sep., Arcidosso, Italy.